

Ginsenoside Rg2 Attenuates Doxorubicin-induced Cardiomyocyte Apoptosis via PI3K/Akt Pathway

Boyong Qiu

Longhua Hospital Shanghai University of Traditional Chinese Medicine

Meijiao Mao

Longhua Hospital Shanghai University of Traditional Chinese Medicine

Shuai Zhang

Longhua Hospital Shanghai University of Traditional Chinese Medicine

Bing Deng

Longhua Hospital Shanghai University of Traditional Chinese Medicine

Lin Shen

Longhua Hospital Shanghai University of Traditional Chinese Medicine

Ping Zhao

Longhua Hospital Shanghai University of Traditional Chinese Medicine

Duan Zhou

Longhua Hospital Shanghai University of Traditional Chinese Medicine

Yihong Wei (✉ longhuawyh@126.com)

Longhua Hospital Shanghai University of Traditional Chinese Medicine

Research Article

Keywords: Ginsenoside Rg2, cardiomyocyte apoptosis, doxorubicin

Posted Date: February 15th, 2021

DOI: <https://doi.org/10.21203/rs.3.rs-191055/v1>

License:   This work is licensed under a Creative Commons Attribution 4.0 International License.

[Read Full License](#)

Abstract

Doxorubicin (DOX) is an important drug for cancer therapy; however, its use is limited by its cardiotoxicity. Ginsenoside Rg2 is extracted from *Panax ginseng*, which is believed to have cardioprotective properties. However, to date, there have been no reports on whether ginsenoside Rg2 could protect cardiomyocytes against DOX. In this study, we investigated the action and underlying mechanisms of ginsenoside Rg2 upon DOX treatment. This study aimed to explore the cardioprotective effects of ginsenoside Rg2 against DOX treatment. Cell Counting kit-8 was used to determine cell viability and terminal deoxynucleotidyl transferase-mediated dUTP nick-end labeling staining was used to detect apoptotic cells. Western blotting was used to investigate the relevant pathways. LY294002 (LY294), a PI3K inhibitor, was used in this study. We found that ginsenoside Rg2 significantly ($P < 0.01$) neutralized cardiomyocyte apoptosis induced by DOX in a dose-dependent manner, which was blocked by LY294. Moreover, ginsenoside Rg2 upregulated Akt phosphorylation through the PI3K/Akt pathway and inhibited p53 expression. Taken together, Ginsenoside Rg2 attenuates DOX-induced cardiomyocyte apoptosis via the PI3K/Akt pathway.

Introduction

Chinese herbal medicine (CHM), as a complementary and alternative medicine, has been used to treat heart conditions for thousands of years¹. Ginseng, the root of *Panax ginseng*, is a kind of CHM widely used nowadays for its health benefits and as a cardiovascular disease treatment in the United States², Canada³, and Europe⁴. To date, over 100 kinds of ginsenosides have been identified⁵, and many of them have been studied for the treatment of various diseases^{6–10}. Ginsenoside Rg2, a major component of the ginsenoside extracted from *P. ginseng* (Fig. 1). It has various pharmacological functions, such as anti-myocardial fibrosis¹¹, amelioration of vascular dementia^{12,13}, improvement of glucose and fat metabolism¹⁴, and antioxidant¹⁵ and antidepressant¹⁶ effects. However, the effect of ginsenoside Rg2 on myocardial injury protection and its underlying mechanism remain unclear.

Doxorubicin (DOX) is an effective drug for the treatment of malignant neoplasia. However, the application of DOX is limited by its cardiotoxicity. Previous studies have shown that long-term DOX application leads to high morbidity of irreversible and late-onset dilated cardiomyopathy^{17,18}. Therefore, new strategies are needed to control DOX cardiotoxicity and protect cardiac myocytes from damage.

It has been shown that ginsenosides Rg1, Rg3, Rb1, and Rh2^{19–22} could alleviate cardiotoxicity induced by DOX; however, there are no reports on ginsenoside Rg2. In view of previous studies, we hypothesized that ginsenoside Rg2 could have the same effect of attenuating DOX-induced cardiomyocytes apoptosis as other ginsenosides. To test this hypothesis, we examined whether ginsenoside Rg2 is functional in H9c2 cells treated with DOX. The expression of Akt and p53 was determined to demonstrate the possible mechanism of action. We aimed to determine whether Rg2 could protect the cells from apoptosis through the phosphatidylinositol 3-kinase (PI3K)/Akt/p53 signaling pathway.

Results

Ginsenoside Rg2 inhibits cardiomyocyte apoptosis induced by doxorubicin.

We first established a DOX-induced apoptosis model in cardiomyocytes. The cytotoxicity of DOX in H9c2 cells was analyzed using the CCK-8 assay, using the appropriate concentration of DOX (5 μ M) at 24 h (Fig. 2A). The cytotoxicity of ginsenoside Rg2 was also measured using the CCK-8 assay, which demonstrated that the maximum safe concentration was 300 μ M after 24 h of treatment (Fig. 2B). Then we tested the effect of simultaneous ginsenoside Rg2 and DOX treatment in H9c2 cells showing that ginsenoside Rg2 significantly increased the cell viability in a dose-dependent manner (Fig. 2C). To further investigate the effect of simultaneous administration of ginsenoside Rg2 and DOX, H9c2 cells were pretreated with ginsenoside Rg2 (100, 200, and 250 μ M) for 24 h before DOX (5 μ M) treatment followed by TUNEL staining (Fig. 2D).

The results showed that ginsenoside Rg2 notably reduced the apoptotic rate compared with the DOX treated cells alone, and the apoptotic rate was even lower at 200 μ M and 250 μ M than at 100 μ M ginsenoside Rg2 ($P < 0.01$) (Fig. 2E). These data suggested that ginsenoside Rg2 inhibited cardiomyocyte apoptosis against DOX.

Ginsenoside Rg2 inhibits ROS generation induced by doxorubicin.

As excessive ROS are generated by DOX, we then tested ROS content in H9c2 cells after treatment with ginsenoside Rg2 and DOX using the ROS assay kit. We found that, compared with the control group, a higher level of ROS was detected in the DOX ($P < 0.01$) and DOX + Rg2 + LY294 ($P < 0.05$) groups. Meanwhile, ROS was markedly reduced in the DOX + Rg2 group ($P < 0.01$) (Fig. 3A). These results suggest that ginsenoside Rg2 could reduce ROS generation caused by DOX.

Ginsenoside Rg2 inhibits ROS generation and cardiomyocyte apoptosis through the PI3K/Akt pathway.

To further clarify the mechanism by which ginsenoside Rg2 inhibits apoptosis and ROS generation in cardiomyocytes, LY294, an inhibitor of PI3K, was used in the treatment. ROS content was dramatically upregulated in H9c2 cells after DOX treatment, which was distinctly inhibited by ginsenoside Rg2. LY294 notably counteracted the inhibitory effect of ginsenoside Rg2 (Fig. 3A). We found that ginsenoside Rg2 significantly inhibited cardiomyocyte apoptosis induced by DOX, which was suppressed by LY294 (Fig. 3B). These data suggest that the effect of ginsenoside Rg2 on cardiomyocyte apoptosis and ROS generation occurs through the PI3K/Akt pathway.

Ginsenoside Rg2 upregulates Akt phosphorylation through the PI3K/Akt pathway and inhibits p53 expression.

To further reveal the mechanism of action of ginsenoside Rg2 against DOX, the PI3K/Akt/p53 pathway was studied. It was found that Akt did not significantly differ between the DOX and DOX + Rg2 groups, but p-Akt was both upregulated in the DOX group and DOX + Rg2 group, and the value of p-Akt/Akt was notably increased in H9c2 cells when treated with ginsenoside Rg2, which was inhibited by LY294 (Fig. 4A, B). Meanwhile, DOX dramatically increased both p53 and p-p53 expression in H9c2 cells. Simultaneous ginsenoside Rg2 treatment significantly reduced p53 expression ($P < 0.01$) and although it did not significantly inhibit p-p53, a trend could be observed, although not within the function of LY294 (Fig. 4A, B). Taken together, these results indicate that ginsenoside Rg2 upregulates Akt phosphorylation through the PI3K/Akt pathway and inhibits p53 expression.

Discussion

Cancer is one of the main causes of death worldwide, and chemotherapy is an important treatment method. Although DOX is an important chemotherapeutic, it exhibits dose-dependent cardiotoxicity¹⁸. Although the detailed mechanism of DOX-induced cardiac toxicity has not been fully elucidated, numerous studies have indicated that DOX-related myocardial damage is possibly correlated with apoptosis²³, inflammation, oxidative stress, and autophagy^{18,24,25}. It has been reported that after the administration of DOX, excessive ROS are produced in cardiomyocytes, accompanied by the upregulation of p53 and caspase-3, thereby activating apoptotic pathways²⁶⁻³², which eventually lead to cardiac dysfunction.

In our study, we found that DOX led to cardiomyocyte apoptosis and generated ROS at certain concentrations, which was consistent with previous studies. We also found that ginsenoside Rg2 significantly reduced cardiomyocyte apoptosis and ROS generation caused by DOX. Ginsenoside Rg2 is a ginsenoside found in ginseng. As a famous traditional Chinese medicine, ginseng is now widely used to reinforce human endurance and resistance to fatigue and physical stress, owing to its role in improving energy and longevity³³. Many previous studies have demonstrated that ginseng plays a role in immunomodulation, cancer suppression, cardiac protection, and neuroprotection³⁴. For instance, ginsenoside Rg3 can inhibit proliferation³⁵, metastasis, and angiogenesis³⁶, as well as activate apoptosis³⁷ and promote immunoreaction³⁸. Ginsenosides, the main active ingredients of ginseng, have also been shown to have a cardioprotective function⁵. In terms of anti-apoptosis, ginsenoside Rb3 exerted anti-apoptotic effects on cardiomyocytes via the PPAR α pathway³⁹, whereas ginsenoside Rg1 attenuated dopamine-induced apoptosis in PC12 cells by suppressing oxidative stress⁴⁰. Ginsenoside Rd was also reported to attenuate the mitochondria-dependent apoptotic pathway via Akt/GSK-3 β signaling⁴¹. Ginsenoside Rg2 was previously reported to inhibit apoptosis induced by H₂O₂ in H9c2 cells⁴² and ameliorate chemical myocardial ischemia in rats⁴³. In addition, in our study, the anti-apoptotic

function of ginsenoside Rg2 in DOX-treated cells was further confirmed using TUNEL staining. This effect was dose-dependent. Ginsenoside Rg2 was also able to reduce ROS induced by DOX).

To further identify the mechanism of action of ginsenoside Rg2 against DOX, the PI3K/Akt pathway was investigated. The PI3K/Akt pathway is thought to be closely related to differentiation, proliferation, apoptosis, and oxidative stress. Its activation is known to reduce cardiomyocyte apoptosis^{44,45}. p53, a downstream factor of the PI3K/Akt pathway, is a classic tumor suppressor and its activation has been reported to accelerate cardiomyocyte apoptosis⁴⁶⁻⁴⁸. Previous studies have also demonstrated that Akt phosphorylation and p53 inhibition could inhibit DOX-induced cardiomyocyte apoptosis and improve myocardial systolic function^{49,50}. In this study, our data illustrated that the ginsenoside Rg2 inhibition of cardiomyocyte apoptosis induced by DOX was repressed by Ly294. Additionally, the results of our ROS assay were consistent with the CCK-8 assay, which showed that ginsenoside Rg2-induced suppression of DOX-induced ROS significantly inhibited Ly294. In addition, western blot analysis indicated that ginsenoside Rg2 notably upregulated p-Akt and p-Akt/t-Akt, which was also suppressed by Ly294. These results demonstrated that the effect of ginsenoside Rg2 against DOX was mediated through the PI3K/Akt pathway. Consistently, in a mouse model of myocardial infarction, ginsenoside Rg2 was also shown to improve cardiac function by promoting Akt phosphorylation¹¹. Our results also showed that DOX significantly upregulated p53 expression, which was remarkably inhibited by ginsenoside Rg2. Although no significant difference was observed in the levels of p-p53 upon ginsenoside Rg2 treatment, there was a downregulation trend. However, it is unclear whether Ly294 represses the expression of p53 and p-p53 and elevates p-p53/p53. Our results demonstrated that ginsenoside Rg2 could downregulate DOX-induced p53 and p-p53, but the underlying mechanism that involves the PI3K/Akt pathway is still unclear, and further study is needed.

In conclusion, this study is the first to report that ginsenoside Rg2 can potentially suppress DOX-triggered cardiotoxicity. Protection of ginsenoside Rg2 against DOX was shown to be associated with decreased production of ROS, downregulation of p53, and increased Akt phosphorylation. The attenuation of DOX-induced cardiomyocyte apoptosis triggered by ginsenoside Rg2 was mediated by the PI3K/Akt pathway. The underlying mechanism involving the PI3K/Akt pathway remains to be further explored. Given the anti-tumor effects of ginsenoside, it is hoped that the application of ginsenoside Rg2 in combination with DOX will improve cardiotoxicity and inhibit tumor cell activity at the same time.

Materials And Methods

Chemicals and reagents.

Ginsenoside Rg2 (purity of 98.18%) was obtained from Manster Biotechnology (Chengdu, China). The rat myocardial cell line H9c2 was acquired from the Cell Resource Center of the Shanghai Institute of Life Sciences, Chinese Academy of Sciences. Enhanced Cell Counting kit-8 (CCK-8), terminal deoxynucleotidyl transferase-mediated dUTP nick-end labeling (TUNEL) one-step apoptosis assay kit, immune staining fix solution, enhanced immunostaining permeabilization solution, reactive oxygen species (ROS) assay kit,

RIPA lysis buffer, bicinchoninic acid (BCA) protein concentration determination kit, sodium dodecyl sulfate polyacrylamide gel electrophoresis (SDS-PAGE) gel preparation kit, SDS-PAGE loading buffer, SDS-PAGE electrophoresis buffer with Tris-Gly, western transfer liquid, BeyoECL Star detection kit, and LY294002 (LY294) were all purchased from Beyotime Technology (Shanghai, China). Multicolor prestained protein ladder and protein sample loading buffer were obtained from Epizyme Biotechnology (Shanghai, China). Dulbecco's modified Eagle's medium (DMEM), fetal bovine serum (FBS), 0.25% trypsin-EDTA, penicillin-streptomycin (P-S), and phosphate buffered saline (PBS) were purchased from Gibco (Waltham, MA, USA), whereas doxorubicin (DOX) and dimethyl sulfoxide (DMSO) were purchased from Sigma-Aldrich (San Luis, MO, USA). Polyvinylidene difluoride (PVDF) was obtained from Merck Chemical Technology (Shanghai, China). Antibodies against Akt, p-Akt, p53, p-p53, and GAPDH were acquired from Cell Signaling Technology (Danvers, MA, USA).

Cell culture.

H9c2 cells were cultured in DMEM containing 10% FBS and 1% P-S at 37 °C in a 5% CO₂ incubator. H9c2 cells were treated with 0.25% trypsin at 80% confluency and passaged at a 1:4 ratio approximately every three days. The cells used in subsequent experiments were in the logarithmic growth phase.

Cell cytotoxicity assay.

H9c2 cells were seeded in 96-well plates at a density of 1×10^4 cells/well and incubated at 37°C for 24 h. The cells were then treated with different concentrations of DOX (2.5, 5, 10, 15, and 20 μ M) and ginsenoside Rg2 (200, 250, 300, 350, and 400 μ M) for another 24 h. After that, the cell supernatant was replaced with 10% CCK-8 diluent and incubated at 37°C for 1 h before the CCK-8 assay was performed. The absorbance value was measured at 450 nm using a multifunctional enzyme standard instrument (SYNERGY H1, BioTek).

To investigate the effect of ginsenoside Rg2 on DOX-induced cardiomyocyte apoptosis, H9c2 cells were first treated with ginsenoside Rg2 for 24 h followed by the addition of DOX for another 24 h. Thereafter, the CCK-8 assay was performed. To determine the underlying mechanism, H9c2 cells were pre-treated with LY294 (1 μ M), a PI3K inhibitor, for 30 min before ginsenoside Rg2 intervention.

Apoptosis assay.

TUNEL staining was used to detect morphological features of apoptosis. After treatment with different concentrations (100, 200, and 250 μ M) of ginsenoside Rg2 for 24 h, H9c2 cells were treated with DOX (5 μ M) for another 24 h. Next, the cell supernatant was replaced with immune staining fix solution for 30 min. After washing with PBS, the cells were mixed with enhanced immunostaining permeabilization

solution for 5 min. The TUNEL solution was then added to the cells and incubated for 60 min at 37 °C, followed by detection using a 200-fold fluorescence microscope (Olympus BX50, Tokyo, Japan).

ROS assay.

The ROS assay kit was used to analyze ROS levels in cardiomyocytes. H9c2 cells were seeded in 96-well plates at a density of 1×10^4 cells/well. After intervention with ginsenoside Rg2, DOX, and LY294, DCFH-DA (10 μ M) was added to the cells, followed by incubation for 20 min at 37 °C. The cells were then washed three times with DMEM and ROS absorbance was measured at 488 nm using a multifunctional enzyme standard instrument.

Western blot analysis.

Briefly, the total proteins of H9c2 cells were extracted according to the manufacturer's instructions. The protein concentration was calculated using the BCA kit. After denaturation at 95°C for 5 min, proteins were separated via SDS-PAGE (10% separating gel and 5% stacking gel, 60 v for 30 min, 100 V for 1 h). The separated proteins were transferred to PVDF membranes at 350 mA for 1 h. Protein ladder markers were used to observe the molecular weight positions. The membranes were pre-incubated in blocking buffer-TBST containing 5% skim milk (w/v) for 1 h at room temperature (nearly 20°C) and then incubated overnight at 4°C with primary antibodies at a dilution of 1:1000. After washing with TBST, the membranes were incubated with a secondary antibody (1:2000 dilution) for 1 h at room temperature. Protein bands were detected using the ECL chemiluminescence system and a gel imaging system (Chemiscope 6300). ImageJ software was used for the gray value statistics. GAPDH was used as the loading control.

Statistical analysis.

All data are presented as mean \pm standard deviation and were analyzed using SPSS Statistics 25. An independent sample t-test was used to compare the two groups. The comparison among the three groups (above) was performed via one-way analysis of variance and the least significant difference test was performed between groups. Non-normal distribution was represented by the median, and the rank sum test was adopted. Statistical significance was assumed if *P* reached a value < 0.05 . Graphs were created using GraphPad Prism 7.0.

Declarations

Data Availability

The data used to support the findings of the study are included within the article.

Conflicts of Interest

The authors have no conflicts of interest to disclose.

Funding Statement

This work was supported by the National Natural Science Foundation of China (No. 81804010).

Author Contributions

Boyong Qiu conducted the experiments and draft the manuscript. Meijiao Mao and Shuai Zhang collected and analyzed the data. Bing Deng, Lin Shen, Ping Zhao and Duan Zhou reviewed and edited the manuscript. Yihong Wei and Ping Zhao conceived of the study and designed the study. All authors have read and approved the final manuscript.

Statement of Informed Consent

There are no human subjects in this article and informed consent is not applicable.

References

1. Hao, P. P. *et al.* Traditional Chinese Medicine for Cardiovascular Disease Evidence and Potential Mechanisms. *J. Am. Coll. Cardiol.* **69**, 2952–2966 <https://doi.org/10.1016/j.jacc.2017.04.041> (2017).
2. Kaufman, D. W., Kelly, J. P., Rosenberg, L., Anderson, T. E. & Mitchell, A. A. Recent patterns of medication use in the ambulatory adult population of the United States - The Slone survey. *JAMA-J. Am. Med. Assoc.* **287**, 337–344 <https://doi.org/10.1001/jama.287.3.337> (2002).
3. Pharand, C. *et al.* Use of OTC and herbal products in patients with cardiovascular disease. *Ann. Pharmacother.* **37**, 899–904 <https://doi.org/10.1345/aph.1C163> (2003).
4. Nilsson, M., Trehn, G. & Asplund, K. Use of complementary and alternative medicine remedies in Sweden. A population-based longitudinal study within the northern Sweden MONICA Project. *J. Intern. Med.* **250**, 225–233 <https://doi.org/10.1046/j.1365-2796.2001.00882.x> (2001).
5. Shi, Z. Y., Zeng, J. Z. & Wong, A. S. T. Chemical Structures and Pharmacological Profiles of Ginseng Saponins. *Molecules (Basel, Switzerland)*. **24**, <https://doi.org/10.3390/molecules24132443> (2019).
6. Cheng, Y., Shen, L. H. & Zhang, J. T. Anti-amnestic and anti-aging effects of ginsenoside Rg1 and Rb1 and its mechanism of action. *Acta Pharmacol. Sin.* **26**, 143–149 <https://doi.org/10.1111/j.1745-7254.2005.00034.x> (2005).

7. Ye, R. *et al.* Ginsenoside Rd attenuates redox imbalance and improves stroke outcome after focal cerebral ischemia in aged mice. *Neuropharmacology*. **61**, 815–824 <https://doi.org/10.1016/j.neuropharm.2011.05.029> (2011).
8. Shin, E. J. *et al.* Ginsenoside Re Rescues Methamphetamine-Induced Oxidative Damage, Mitochondrial Dysfunction, Microglial Activation, and Dopaminergic Degeneration by Inhibiting the Protein Kinase C delta Gene. *Mol. Neurobiol.* **49**, 1400–1421 <https://doi.org/10.1007/s12035-013-8617-1> (2014).
9. He, B. C. *et al.* Ginsenoside Rg3 inhibits colorectal tumor growth through the down-regulation of Wnt/beta-catenin signaling. *International Journal of Oncology*. **38**, 437–445 <https://doi.org/10.3892/ijo.2010.858> (2011).
10. Huang, G. X. *et al.* Ginsenosides Rb3 and Rd reduce polyps formation while reinstate the dysbiotic gut microbiota and the intestinal microenvironment in Apc(Min/+) mice. *Sci Rep.* **7**, 14 <https://doi.org/10.1038/s41598-017-12644-5> (2017).
11. Li, X., Xiang, N. & Wang, Z. Ginsenoside Rg2 attenuates myocardial fibrosis and improves cardiac function after myocardial infarction via AKT signaling pathway. *Bioscience, biotechnology, and biochemistry*. **84**, 2199–2206 <https://doi.org/10.1080/09168451.2020.1793292> (2020).
12. Cui, J. *et al.* Ginsenoside Rg2 protects PC12 cells against β -amyloid(25–35)-induced apoptosis via the phosphoinositide 3-kinase/Akt pathway. *Chemico-biological interactions*. **275**, 152–161 <https://doi.org/10.1016/j.cbi.2017.07.021> (2017).
13. Zhang, G. *et al.* Panax ginseng ginsenoside-Rg2 protects memory impairment via anti-apoptosis in a rat model with vascular dementia. *J Ethnopharmacol.* **115**, 441–448 <https://doi.org/10.1016/j.jep.2007.10.026> (2008).
14. Cheng, B. *et al.* Ginsenoside Rg2 Ameliorates High-Fat Diet-Induced Metabolic Disease through SIRT1. *Journal of agricultural and food chemistry*. **68**, 4215–4226 <https://doi.org/10.1021/acs.jafc.0c00833> (2020).
15. Kang, H. J. *et al.* Stereospecificity of ginsenoside Rg2 epimers in the protective response against UV-B radiation-induced oxidative stress in human epidermal keratinocytes. *Journal of photochemistry and photobiology. B, Biology*. **165**, 232–239 <https://doi.org/10.1016/j.jphotobiol.2016.10.034> (2016).
16. Ren, Y. *et al.* Antidepressant-like effects of ginsenoside Rg2 in a chronic mild stress model of depression. *Brain research bulletin*. **134**, 211–219 <https://doi.org/10.1016/j.brainresbull.2017.08.009> (2017).
17. Wallace, K. B. Doxorubicin-induced cardiac mitochondrionopathy. *Pharmacology & toxicology*. **93**, 105–115 <https://doi.org/10.1034/j.1600-0773.2003.930301.x> (2003).
18. Zhang, Y. W., Shi, J., Li, Y. J. & Wei, L. Cardiomyocyte death in doxorubicin-induced cardiotoxicity. *Archivum immunologiae et therapiae experimentalis*. **57**, 435–445 <https://doi.org/10.1007/s00005-009-0051-8> (2009).

19. Xu, Z. M., Li, C. B., Liu, Q. L., Li, P. & Yang, H. Ginsenoside Rg1 Prevents Doxorubicin-Induced Cardiotoxicity through the Inhibition of Autophagy and Endoplasmic Reticulum Stress in Mice. *International journal of molecular sciences*. **19**, <https://doi.org/10.3390/ijms19113658> (2018).
20. Li, L. *et al.* Ginsenoside Rg3 micelles mitigate doxorubicin-induced cardiotoxicity and enhance its anticancer efficacy. *Drug delivery*. **24**, 1617–1630 <https://doi.org/10.1080/10717544.2017.1391893> (2017).
21. Zhang, Y. *et al.* Ginsenoside Rb1 Inhibits Doxorubicin-Triggered H9C2 Cell Apoptosis via Aryl Hydrocarbon Receptor. *Biomolecules & therapeutics*. **25**, 202–212 <https://doi.org/10.4062/biomolther.2016.066> (2017).
22. Wang, H. *et al.* Cardioprotective Effects of 20(S)-Ginsenoside Rh2 against Doxorubicin-Induced Cardiotoxicity In Vitro and In Vivo. *Evidence-based complementary and alternative medicine: eCAM* 2012, 506214, doi:10.1155/2012/506214 (2012).
23. Kalyanaraman, B. *et al.* Doxorubicin-induced apoptosis: implications in cardiotoxicity. *Molecular and cellular biochemistry*. **234–235**, 119–124 (2002).
24. Zhang, J. *et al.* Protective effects of tannic acid on acute doxorubicin-induced cardiotoxicity: Involvement of suppression in oxidative stress, inflammation, and apoptosis. *Biomedicine & pharmacotherapy = Biomedecine & pharmacotherapie*. **93**, 1253–1260 <https://doi.org/10.1016/j.biopha.2017.07.051> (2017).
25. Mantawy, E. M., El-Bakly, W. M., Esmat, A., Badr, A. M. & El-Demerdash, E. Chrysin alleviates acute doxorubicin cardiotoxicity in rats via suppression of oxidative stress, inflammation and apoptosis. *European journal of pharmacology*. **728**, 107–118 <https://doi.org/10.1016/j.ejphar.2014.01.065> (2014).
26. Kotamraju, S., Konorev, E. A., Joseph, J. & Kalyanaraman, B. Doxorubicin-induced apoptosis in endothelial cells and cardiomyocytes is ameliorated by nitron spin traps and ebselen. Role of reactive oxygen and nitrogen species. *The Journal of biological chemistry*. **275**, 33585–33592 <https://doi.org/10.1074/jbc.M003890200> (2000).
27. Zhang, Y. Y., Yi, M. & Huang, Y. P. Oxymatrine Ameliorates Doxorubicin-Induced Cardiotoxicity in Rats. *Cellular physiology and biochemistry: international journal of experimental cellular physiology, biochemistry, and pharmacology*. **43**, 626–635 <https://doi.org/10.1159/000480471> (2017).
28. Khafaga, A. F. & El-Sayed, Y. S. All-trans-retinoic acid ameliorates doxorubicin-induced cardiotoxicity: in vivo potential involvement of oxidative stress, inflammation, and apoptosis via caspase-3 and p53 down-expression. *Naunyn-Schmiedeberg's archives of pharmacology*. **391**, 59–70 <https://doi.org/10.1007/s00210-017-1437-5> (2018).
29. Shizukuda, Y., Matoba, S., Mian, O. Y., Nguyen, T. & Hwang, P. M. Targeted disruption of p53 attenuates doxorubicin-induced cardiac toxicity in mice. *Molecular and cellular biochemistry*. **273**, 25–32 <https://doi.org/10.1007/s11010-005-5905-8> (2005).
30. Yeh, P. Y. *et al.* Phosphorylation of p53 on Thr55 by ERK2 is necessary for doxorubicin-induced p53 activation and cell death. *Oncogene*. **23**, 3580–3588 <https://doi.org/10.1038/sj.onc.1207426> (2004).

31. Wu, W. *et al.* Expression of constitutively active phosphatidylinositol 3-kinase inhibits activation of caspase 3 and apoptosis of cardiac muscle cells. *The Journal of biological chemistry*. **275**, 40113–40119 <https://doi.org/10.1074/jbc.M004108200> (2000).
32. Wang, G. W., Klein, J. B. & Kang, Y. J. Metallothionein inhibits doxorubicin-induced mitochondrial cytochrome c release and caspase-3 activation in cardiomyocytes. *The Journal of pharmacology and experimental therapeutics*. **298**, 461–468 (2001).
33. Liu, C. X. & Xiao, P. G. Recent advances on ginseng research in China. *J Ethnopharmacol*. **36**, 27–38 [https://doi.org/10.1016/0378-8741\(92\)90057-x](https://doi.org/10.1016/0378-8741(92)90057-x) (1992).
34. Xiang, Y. Z., Shang, H. C., Gao, X. M. & Zhang, B. L. A comparison of the ancient use of ginseng in traditional Chinese medicine with modern pharmacological experiments and clinical trials. *Phytotherapy research: PTR*. **22**, 851–858 <https://doi.org/10.1002/ptr.2384> (2008).
35. Wang, L. *et al.* Ginsenoside Rg3 sensitizes human non-small cell lung cancer cells to γ -radiation by targeting the nuclear factor- κ B pathway. *Mol Med Rep*. **12**, 609–614 <https://doi.org/10.3892/mmr.2015.3397> (2015).
36. Mochizuki, M. *et al.* Inhibitory effect of tumor metastasis in mice by saponins, ginsenoside-Rb2, 20(R)- and 20(S)-ginsenoside-Rg3, of red ginseng. *Biological & pharmaceutical bulletin*. **18**, 1197–1202 <https://doi.org/10.1248/bpb.18.1197> (1995).
37. Zhang, F. *et al.* 20(S)-ginsenoside Rg3 promotes senescence and apoptosis in gallbladder cancer cells via the p53 pathway. *Drug design, development and therapy*. **9**, 3969–3987 <https://doi.org/10.2147/dddt.S84527> (2015).
38. Sun, M. *et al.* Anticancer effects of ginsenoside Rg3 (Review). *International journal of molecular medicine*. **39**, 507–518 <https://doi.org/10.3892/ijmm.2017.2857> (2017).
39. Chen, X. *et al.* Ginsenoside Rb3 regulates energy metabolism and apoptosis in cardiomyocytes via activating PPAR α pathway. *Biomedicine & pharmacotherapy = Biomedecine & pharmacotherapie*. **120**, 109487 <https://doi.org/10.1016/j.biopha.2019.109487> (2019).
40. Chen, X. C. *et al.* Ginsenoside Rg1 attenuates dopamine-induced apoptosis in PC12 cells by suppressing oxidative stress. *European journal of pharmacology*. **473**, 1–7 [https://doi.org/10.1016/s0014-2999\(03\)01945-9](https://doi.org/10.1016/s0014-2999(03)01945-9) (2003).
41. Wang, Y. *et al.* Ginsenoside Rd attenuates myocardial ischemia/reperfusion injury via Akt/GSK-3 β signaling and inhibition of the mitochondria-dependent apoptotic pathway. *PloS one*. **8**, e70956 <https://doi.org/10.1371/journal.pone.0070956> (2013).
42. Fu, W. *et al.* Protective effects of ginsenoside Rg2 against H₂O₂-induced injury and apoptosis in H9c2 cells. *International journal of clinical and experimental medicine*. **8**, 19938–19947 (2015).
43. Tian, J. M. *et al.* [Effect of ginsenoside Rg2 on chemical myocardial ischemia in rats]. *Zhongguo Zhong yao za zhi = Zhongguo zhongyao zazhi = China journal of Chinese materia medica*. **28**, 1191–1192 (2003).
44. Yu, W. *et al.* Apigenin Attenuates Adriamycin-Induced Cardiomyocyte Apoptosis via the PI3K/AKT/mTOR Pathway. *Evidence-based complementary and alternative medicine: eCAM* 2017,

2590676, doi:10.1155/2017/2590676 (2017).

45. Shu, Z. *et al.* Cardioprotective effects of dihydroquercetin against ischemia reperfusion injury by inhibiting oxidative stress and endoplasmic reticulum stress-induced apoptosis via the PI3K/Akt pathway. *Food & function*. **10**, 203–215 <https://doi.org/10.1039/c8fo01256c> (2019).
46. Sun, A. *et al.* Mitochondrial aldehyde dehydrogenase 2 plays protective roles in heart failure after myocardial infarction via suppression of the cytosolic JNK/p53 pathway in mice. *Journal of the American Heart Association*. **3**, e000779 <https://doi.org/10.1161/jaha.113.000779> (2014).
47. Crighton, D. *et al.* DRAM, a p53-induced modulator of autophagy, is critical for apoptosis. *Cell* **126**, 121–134, doi:10.1016/j.cell.2006.05.034 (2006).
48. Bensaad, K. *et al.* TIGAR, a p53-inducible regulator of glycolysis and apoptosis. *Cell*. **126**, 107–120 <https://doi.org/10.1016/j.cell.2006.05.036> (2006).
49. Chen, R. C. *et al.* Total Flavonoids from *Clinopodium chinense* (Benth.) O. Ktze Protect against Doxorubicin-Induced Cardiotoxicity In Vitro and In Vivo. *Evidence-based complementary and alternative medicine: eCAM* 2015, 472565, doi:10.1155/2015/472565 (2015).
50. Hong, H. J. *et al.* Tanshinone IIA prevents doxorubicin-induced cardiomyocyte apoptosis through Akt-dependent pathway. *International journal of cardiology*. **157**, 174–179 <https://doi.org/10.1016/j.ijcard.2010.12.012> (2012).

Figures

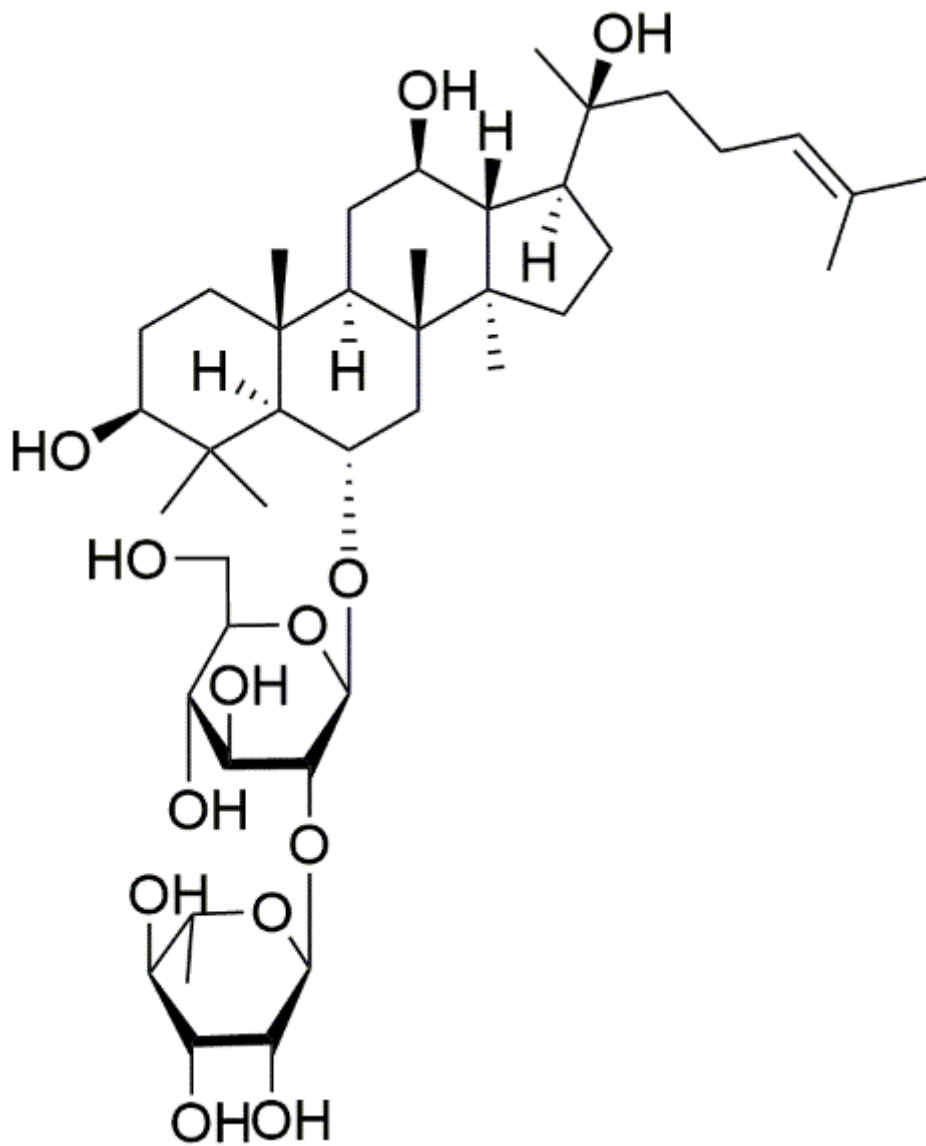


Figure 1

Chemical structure of Ginsenoside Rg2. The formula of Rg2 is $C_{42}H_{72}O_{13}$ and its molecular weight is 785.03.

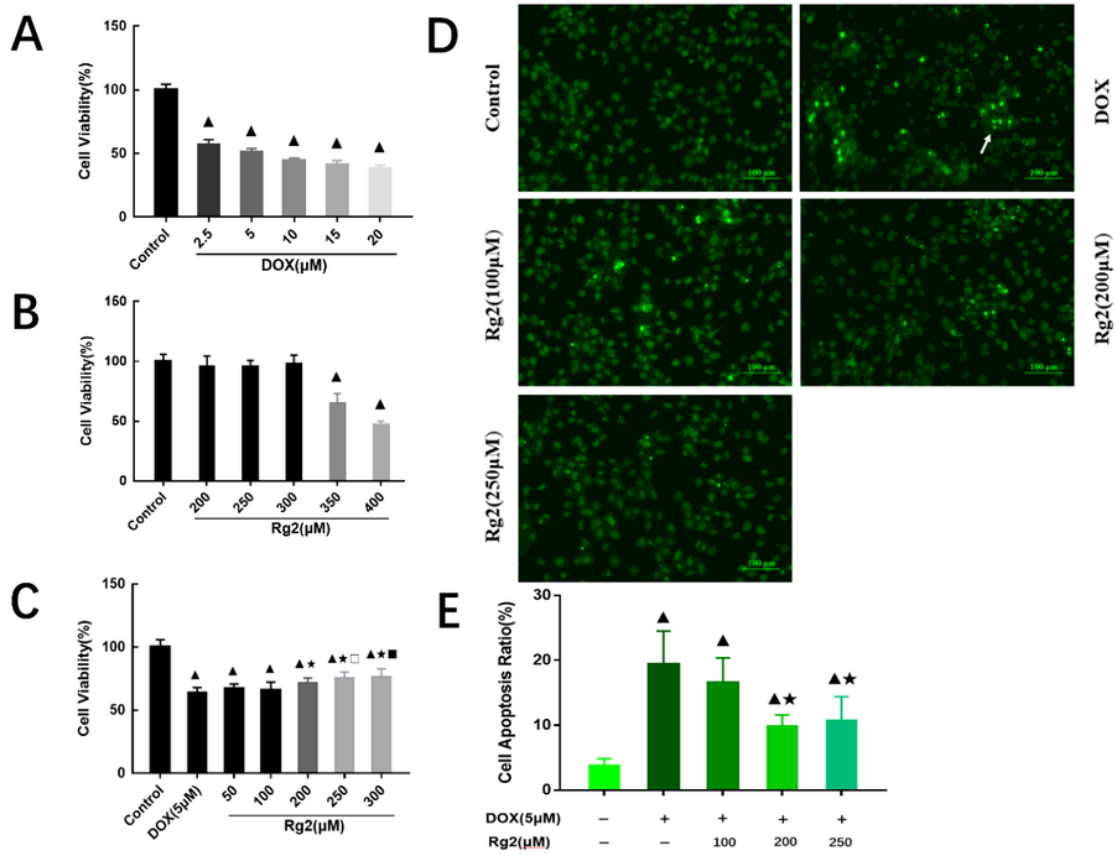


Figure 2

Ginsenoside Rg2 neutralized DOX-induced cardiomyocyte apoptosis. CCK-8 was used to measure H9c2 cells viability under the influence of DOX (A), Rg2 (B), and DOX with different concentrations of Rg2 (C). Morphological features of cell apoptosis in H9c2 cells were detected via TUNEL staining, in green (D), and cell apoptosis ratio was calculated using ImageJ (E). The scale is 100 μm in picture D, and the white arrow points to the bright apoptotic cells. \blacktriangle $P < 0.01$ vs Control group; \boxtimes $P < 0.01$ vs DOX group; \square $P < 0.05$ and \blacksquare $P < 0.01$ vs Rg2 (200 μM) group.

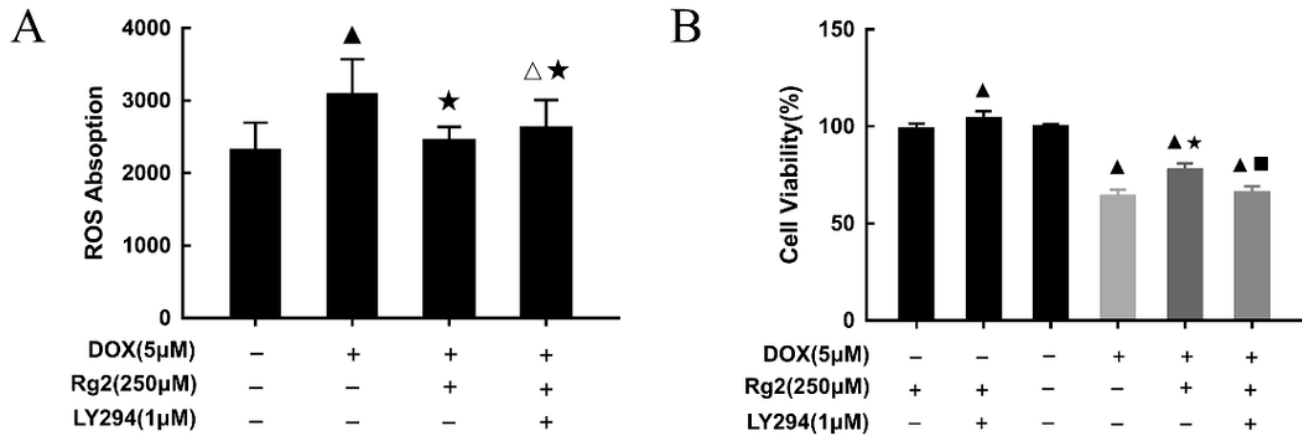


Figure 3

Ginsenoside Rg2 decreased ROS generation and apoptosis through PI3K/Akt pathway. (A) ROS assay was used to test the expression of ROS absorption. (B) CCK-8 assay was used to detect the cell viability. ▲P <0.01 and △P <0.05 vs Control group; ☒P <0.01 vs DOX group; ■P <0.01 vs Rg2 (250 μM) group.

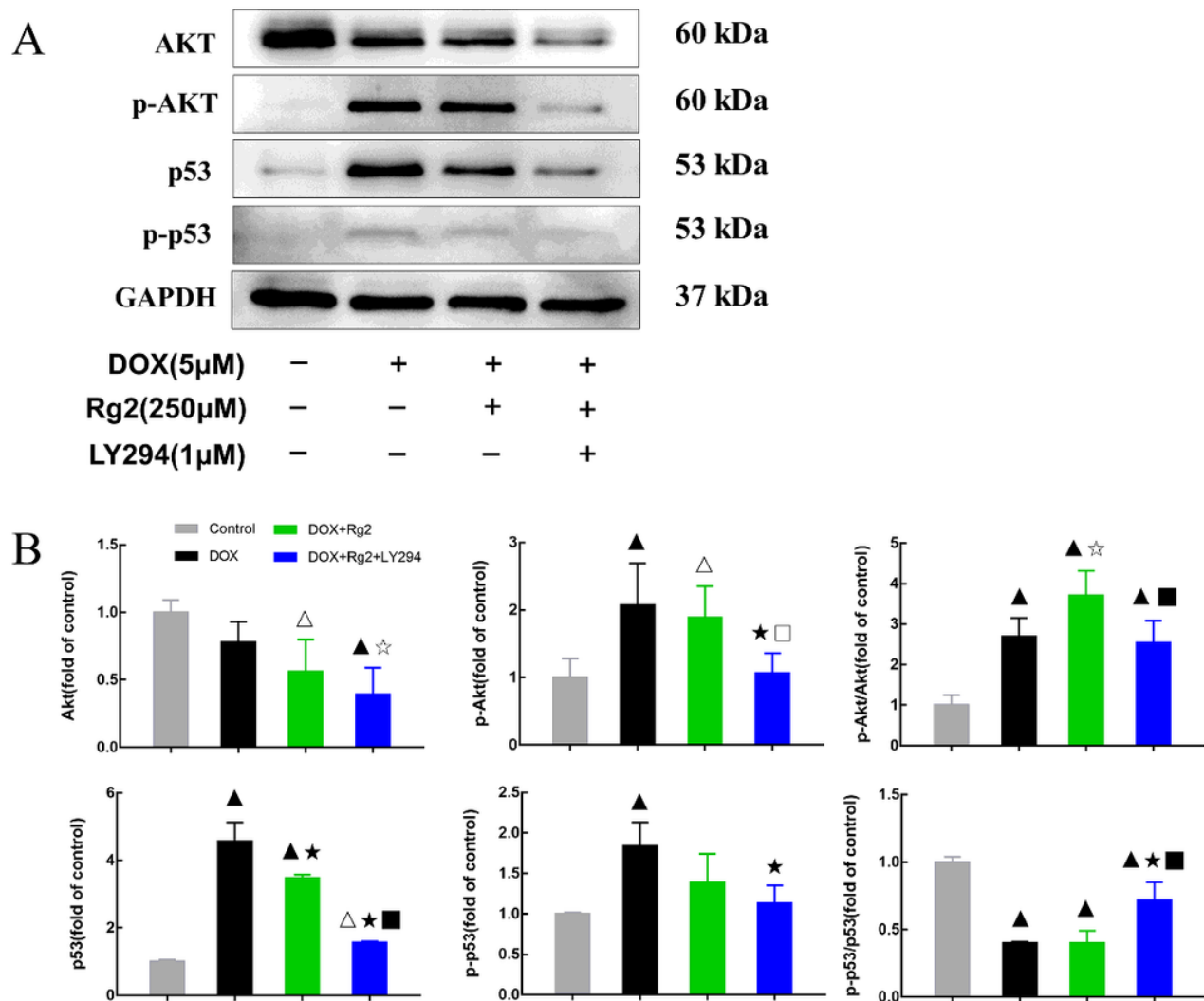


Figure 4

Ginsenoside Rg2 upregulated Akt phosphorylation and inhibited DOX upregulation of p53 expression. (A) The level of Akt, p-Akt, p53 and p-p53 proteins in H9c2 cells was detected via western blotting. (B) ImageJ was used to measure the gray value of strip. ▲P < 0.01 and △P < 0.05 vs Control group; ☆P < 0.01 and ★P < 0.05 vs DOX group; □P < 0.05 and ■P < 0.01 vs DOX+Rg2 group (n=3-4).

Supplementary Files

This is a list of supplementary files associated with this preprint. Click to download.

- [Supplementaryblots.docx](#)